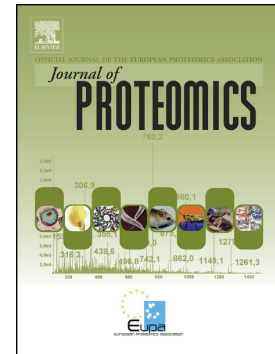


Accepted Manuscript

Defining the pathogenic threat of envenoming by south african shield-nosed and coral snakes (genus aspidelaps), and revealing the likely efficacy of available antivenom

Gareth Whiteley, Nicholas R. Casewell, Davinia PLA, Sarai Quesada-Bernat, Rhiannon A.E. Logan, Fiona M.S. Bolton, Simon C. Wagstaff, José M. Gutiérrez, Juan J. Calvete, Robert A. Harrison



PII: S1874-3919(18)30360-9
DOI: doi:[10.1016/j.jprot.2018.09.019](https://doi.org/10.1016/j.jprot.2018.09.019)
Reference: JPROT 3225
To appear in: *Journal of Proteomics*
Received date: 25 July 2018
Revised date: 15 September 2018
Accepted date: 30 September 2018

Please cite this article as: Gareth Whiteley, Nicholas R. Casewell, Davinia PLA, Sarai Quesada-Bernat, Rhiannon A.E. Logan, Fiona M.S. Bolton, Simon C. Wagstaff, José M. Gutiérrez, Juan J. Calvete, Robert A. Harrison , Defining the pathogenic threat of envenoming by south african shield-nosed and coral snakes (genus aspidelaps), and revealing the likely efficacy of available antivenom. Jprot (2018), doi:[10.1016/j.jprot.2018.09.019](https://doi.org/10.1016/j.jprot.2018.09.019)

This is a PDF file of an unedited manuscript that has been accepted for publication. As a service to our customers we are providing this early version of the manuscript. The manuscript will undergo copyediting, typesetting, and review of the resulting proof before it is published in its final form. Please note that during the production process errors may be discovered which could affect the content, and all legal disclaimers that apply to the journal pertain.

Defining the pathogenic threat of envenoming by south african shield-nosed and coral snakes (genus *Aspidelaps*), and revealing the likely efficacy of available antivenom

Gareth Whiteley^{1,#}, Nicholas R. Casewell^{1,#}, Davinia PLA², Sarai Quesada-Bernat², Rhiannon A. E. Logan¹, Fiona M. S. Bolton¹, Simon C. Wagstaff³, José M. Gutiérrez⁴, Juan J. Calvete^{2,*}, Robert A. Harrison^{1,*}

¹ Alistair Reid Venom Research Unit, Parasitology Department, Liverpool School of Tropical Medicine, Pembroke Place, Liverpool, L3 5QA, UK. Emails: garethwhiteleymsc@yahoo.com; nicholas.casewell@lstmed.ac.uk; rhiannon.logan@lstmed.ac.uk; fiona.bolton@lstmed.ac.uk; robert.harrison@lstmed.ac.uk

² Evolutionary and Translational Venomics Laboratory, CSIC, Jaime Roig 11, 46010 Valencia, Spain. Emails: dpla@ibv.csic.es; jcalvete@ibv.csic.es; squesada@ibv.csic.es

³ Bioinformatics Unit, Liverpool School of Tropical Medicine, Pembroke Place, Liverpool, L3 5QA, UK. Email: simon.wagstaff@lstmed.ac.uk

⁴ Instituto Clodomiro Picado, Facultad de Microbiología, Universidad de Costa Rica, San José, 11501-2060, Costa Rica. Email: jose.gutierrez@ucr.ac.cr

Joint first authors

* Corresponding authors:

- Juan J Calvete: jcalvete@ibv.csic.es
- Robert A. Harrison: robert.harrison@lstmed.ac.uk

Keywords: Snake venom proteome; snake venom gland transcriptomics; South african shield-nosed and coral snakes; genus *Aspidelaps*; *Aspidelaps* venoms toxicity; third-generation antivenomics; *in vitro* and *in vivo* preclinical assays.

ABSTRACT

While envenoming by the southern African shield-nosed or coral snakes (genus *Aspidelaps*) has caused fatalities, bites are uncommon. Consequently, this venom is not used in the mixture of snake venoms used to immunise horses for the manufacture of regional SAIMR (South African Institute for Medical Research) polyvalent antivenom. *Aspidelaps* species are even excluded from the manufacturer's list of venomous snakes that can be treated by this highly effective product. This leaves clinicians, albeit rarely, in a therapeutic vacuum when treating envenoming by these snakes. This is a significantly understudied small group of nocturnal snakes and little is known about their venom compositions and toxicities. Using a murine preclinical model, this study determined that the paralysing toxicity of venoms from *Aspidelaps scutatus intermedius*, *A. lubricus cowlesi* and *A. l. lubricus* approached that of venoms from highly neurotoxic African cobras and mambas. This finding was consistent with the cross-genus dominance of venom three-finger toxins, including numerous isoforms which showed extensive interspecific variation. Our comprehensive analysis of venom proteomes showed that the three *Aspidelaps* species possess highly similar venom proteomic compositions. We also revealed that the SAIMR polyvalent antivenom cross-reacted extensively *in vitro* with venom proteins of the three *Aspidelaps*. Importantly, this cross-genus venom-IgG binding translated to preclinical (in a murine model) neutralisation of *A. s. intermedius* venom-induced lethality by the SAIMR polyvalent antivenom, at doses comparable with those that neutralise venom from the cape cobra (*Naja nivea*), which the antivenom is directed against. Our results suggest a wider than anticipated clinical utility of the SAIMR polyvalent antivenom, and here we seek to inform southern African clinicians that this readily available antivenom is likely to prove effective for victims of *Aspidelaps* envenoming.

INTRODUCTION

The 81,000-138,000 estimates of the global mortality caused by snake envenoming include between 20,000-32,000 deaths in sub-Saharan Africa [1]. While the coagulopathic and haemorrhagic consequences of envenoming by *Echis ocellatus* saw-scaled (or carpet) vipers in West Africa and *Bitis arietans* puff adders throughout Africa account for most deaths, fatal envenoming by several neurotoxic *Naja* species of cobras and *Dendroaspis* species of mambas are also commonly reported [2]. Owing to the frequency of severe and fatal envenoming by these diverse snake species, their venoms are often mixed to hyper-immunise horses or sheep for the manufacture of polyspecific antivenom IgG to treat patients. The need to tailor antivenom production to envenoming by the most medically-important snakes, coupled with the costs of venom production and antivenom manufacture, typically translates to a lack of antivenom manufactured to treat tropical snake species that pose a relatively low mortality/morbidity risk.

The *Aspidelaps* coral and shield-nosed snakes of southern Africa is one such genus – none of the antivenoms manufactured for Africa include this venom in their manufacture [3] (WHO database <http://apps.who.int/bloodproducts/snakeantivenoms/database/>). Documented human fatalities, although rare, have occurred from both *A. lubricus* and *A. scutatus* [4, 5] and identify neurotoxic manifestations. In one case study, a 4-year-old female child who was bitten by a juvenile *A. scutatus* snake, became sub-comatose within two hours and was hyper-salivating and dysphonic. Respiratory collapse followed half an hour later and required mechanical ventilation but showed little improvement. Subsequently, the child did not survive a sudden cardiac arrest 16 hours post-envenomation [6]. In a second, a 30-year-old male bitten on the finger by a shield-nosed snake presented with symptoms of neurotoxicity, including progressive slurring of speech, drooping of both eyelids and impairment of respiratory muscles and ultimate recovery [7]. Another bite from a Namibian *A. s. scutatus* produced only cytotoxic symptoms, with swelling of the limb but no necrosis [8]. While a series of insignificant *A. l. lubricus* bites have been also described [9], the deaths of two indigenous Namibian children have been attributed to possible envenoming by *A. l. infuscatus* [5].

Aspidelaps species are relatively small (50-75 cm long), robust and easily recognisable snakes and as a genus their distribution is restricted to Namibia, Botswana, Zimbabwe, Mozambique and South Africa. The name of the *A. lubricus lubricus*, southern coral snake and sub-species (*A. l. infuscatus* (western coral snake) and to a lesser extent, *A. l. cowlesi* (Cowle's shield snake)) reflects their red to orange

scale coloration and black cross-band patterns. The name of the *A. s. scutatus*, shield-nose snake and two sub-species (*A. s. fulafulus* (eastern shield-nose snake) and *A. s. intermedius* (intermediate shield-nose snake)) refer to their much-enlarged rostral scale (for more herpetological detail see [4, 5, 10-13]).

The first toxinological study on *Aspidelaps* venom identified a phospholipase A₂ (PLA₂) as the major component of *A. scutatus* venom [14]. A bibliographic search in PubMed found 10 hits for "*Aspidelaps*" between 1984 and 2018. Four of these papers reported the isolation, primary structures and some properties of *A. scutatus* venom proteins, including PLA₂s CM-I, CM-II [P07037] and CM-III [15] and S₂C₁ and S₂C₂ [16]; long neurotoxin S₄C₆ [P25670] [17]; and putative cytotoxin homologues S₃C₁, S₃C₂ [P19003], S₃C₃, S₄C₁, S₄C₇ and S₄C₈ [P19004] [18].

The i.v. median murine lethal dose (LD₅₀) for *A. scutatus* venom was 11.5-13 µg/mouse [14] and 1.7 ± 0.5 µg/mouse for the isolated PLA₂ proteins, CM-I=CM-II, and 1.1 ± 0.5 µg/mouse for CM-III [15]. The LD₅₀ for the isolated long neurotoxin S₄C₆ (2.2 ± 0.04 µg/mouse) was lower than the cytotoxin homologues (6.6-54 µg/mouse) and the functionally unspecified S₄C₁ (LD₅₀ 3.6 µg/g mouse) and S₄C₇ (LD₅₀ 0.25 µg/g mouse) exhibited, respectively, the lowest and highest toxicity [16-18]. The recorded i.v. venom LD₅₀ of 6 µg/mouse for *A. l. cowlesi* [4, 19] is comparable to those of the Cape cobra (*Naja nivea*, 7 µg/mouse) and black mamba (*Dendroaspis polylepis*, 5 µg/mouse) [20, 21; <http://snakedatabase.org>].

While the above historical literature reveals some penetrating insight to specific venoms and their toxins, there remain significant gaps in our knowledge of this enigmatic genus of venomous snakes. We therefore carried out multidisciplinary, multispecies analyses to define and compare the venom proteomes (underpinned by comprehensive venom gland transcriptomics) of the intermediate shield-nose snake (*A. s. intermedius*), southern coral snake (*A. l. lubricus*), and Cowle's shield snake (*A. l. cowlesi*); assessing the mechanism of action underpinning lethality by *A. s. intermedius* in the murine system, and the neutralisation of its toxicological effects by SAIMR polyvalent antivenom.

EXPERIMENTAL SECTION

Biological materials

Venom was extracted from (i) a single adult specimen of the intermediate shield-nose snake (*Aspidelaps scutatus intermedius*), (ii) six Cowle's shield snakes (*Aspidelaps lubricus cowlesi*), and (iii) four Cape coral snakes (*Aspidelaps lubricus lubricus*). All snakes were captive bred and maintained in individual cages within the temperature, humidity and light-controlled environment of the herpetarium of the Alistair Reid Venom Research Unit at the Liverpool School of Tropical Medicine. This facility and its protocols for the expert husbandry of the snakes is inspected and approved by the UK Home Office and the LSTM Animal Welfare and Ethical Review Board. The number of snakes used in this study was the maximum possible given the limited availability of these animals in our facility. Three days after venom extraction, venom glands were dissected from the single specimen of the intermediate shield-nose snake (*A. s. intermedius*) following terminal anaesthesia (Pentaject), and immediately snap frozen in liquid nitrogen. For immunological analyses we used the SAIMR (South African Institute for Medical Research) polyvalent snake antivenom manufactured by South African Vaccine Producers (Pty), Ltd. (Johannesburg, South Africa). This IgG-derived F(ab')₂ antivenom is made by immunising horses with venom from the following snake species: *Bitis arietans* and *B. gabonica* (family Viperidae) and *Dendroaspis angusticeps*, *D. jamesoni*, *D. polylepis*, *Hemachatus haemachatus*, *Naja annulifera*, *N. melanoleuca*, *N. mossambica* and *N. nivea* (family Elapidae).

Transcriptomics

We constructed the *A. s. intermedius* venom gland transcriptome using the methods previously described by our group [22, 23]. Briefly, the venom gland tissue was homogenised under liquid nitrogen using a pestle and mortar and a TissueRuptor (QIAGEN), and total RNA was extracted using the TRIzol Plus RNA Purification System (ThermoFisher) protocol. The RNA samples were DNase treated (On-Column PureLink DNase; Life Technologies) and total RNA eluted in 30µL nuclease free water (QIAGEN). Total RNA underwent two rounds of poly(A) selection using the Dynabeads mRNA DIRECT purification kit (Life Technologies), and was then eluted in nuclease free water, before the quality and quantity of isolated RNA was assessed using a Bioanalyzer (Agilent). One µL of the resulting total RNA was loaded onto an Agilent RNA 6000 Nano Chip and inserted into the Agilent 5000 Bioanalyzer for analysis. Agilent RNA 2100 Expert software was used to calculate total RNA concentration and

assign a RNA integrity number (RIN) [24]. Subsequently, the sequencing library was prepared using 50 ng of enriched RNA using the Script-Seq v2 RNA-Seq Library Preparation Kit (epicenter), following 12 cycles of amplification. The sequencing library was then purified using AMPure XP beads (Agencourt), quantified using the Qubit dsDNA HS Assay kit (Life Technologies) and the size distribution assessed using a Bioanalyser (Agilent). Sequencing libraries were multiplexed with others not reported in this study, and sequencing performed on an Illumina MiSeq platform using 250bp paired-end reads technology (Centre for Genomics Research, University of Liverpool). The *A. s. intermedius* sample represented 1/6th of this sequencing lane and resulted in 5,664,906 reads. The ensuing read data was quality processed as previously described [22, 23, 25, 26], resulting in the removal of adapter sequences (Cutadapt; <https://code.google.com/p/cutadapt/>) and low quality bases (Sickle; <https://github.com/najoshi/sickle>). Paired-end read data were then assembled into contigs using VTBuilder [27] with the following parameters: min. transcript length 150 bp; min. read length 150bp; min. isoform similarity 96%. As part of this process, the VTBuilder algorithm also generates relative transcript expression data via a normalised read mapping approach [27]. The resulting assembled contigs were annotated using BLAST2GO Pro v3 [28] using the blastx-fast algorithm with a significance threshold of 1e-5 against NCBI's non-redundant (NR) protein database (41 volumes, Nov 2015). Following annotation, contigs were grouped into the following categories: toxins (contigs with blast annotations to sequences previously described as pathogenic toxins), non-toxins (contigs matching other sequences, such as housekeeping genes) and unassigned (those with no matches assigned or hits <1e-5). Where toxin contigs exhibited 100% identity to one another in overlapping regions (>50bp long), indicative of underclustering, the contigs and their expression levels were merged. Raw sequence reads have been deposited in the NCBI sequence read archive (SRA) under accession SRP153153 and linked to the BioProject identifier PRJNA480570. Assembled toxin-coding contigs are found in Supplementary Table S1.

Isolation and proteomics characterisation of venom peptidome and proteome

Two milligrams of crude, lyophilised venom were dissolved in 200 µL of 5% acetonitrile in water containing 0.1% trifluoroacetic acid (TFA), centrifuged to remove debris, and separated by reverse-phase HPLC using a Teknokroma Europa Protein 300 C18 (0.4 cm × 25 cm, 5 µm particle size, 300 Å pore size) column and an LC 1100 High Pressure Gradient System (Agilent Technologies, Santa Clara, CA, USA) equipped with DAD detector and micro-Auto-sampler. The flow-rate was set to 1 mL/min and the

column was developed with a linear gradient of 0.1% TFA in water (solution A) and acetonitrile (solution B) using the following column elution conditions: isocratically (5% B) for 5 min, followed by 5%–25% B for 10 min, 25%–45% B for 60 min, and 45%–70% for 10 min. Protein detection was carried out at 215 nm with a reference wavelength of 400 nm. Fractions were collected manually, dried in a vacuum centrifuge (Savant), redissolved in water, and submitted to electrospray ionisation (ESI) molecular mass determination. To this end, intact peptides and proteins eluted in each RP-HPLC fraction were separated by nano-Acquity UltraPerformance LC[®] (UPLC[®], Waters Corporation, Milford, MA, USA) using BEH130 C18 (100 µm × 100 mm, 1.7 µm particle size) column in-line with a SYNAPT[®] G2 High Definition Mass Spectrometry System (Waters Corp. Milford, MA, USA). The flow rate was set to 0.6 µL/min and the column was developed with a linear gradient of 0.1% formic acid in water (solution A) and 0.1% formic acid in acetonitrile (solution B), isocratically 1% B for 1 min, followed by 1%–12% B for 1 min, 12%–40% B for 15 min, 40%–85% B for 2 min. Isotope-averaged molecular masses were calculated from manually deisotoped and deconvoluted ESI mass spectra.

Chromatographic fractions were also analysed by SDS-PAGE in 15% polyacrylamide gels, under reducing and non-reducing conditions. Gels were stained with Coomassie Brilliant Blue R-250 (Sigma-Aldrich, St. Louis, MO, USA). Electrophoretic protein bands were excised from Coomassie Brilliant Blue-stained SDS-PAGE gels and subjected to in-gel reduction (10 mM dithiothreitol) and alkylation (50 mM iodoacetamide) before overnight sequencing-grade trypsin digestion (66 ng/µL in 25 mM ammonium bicarbonate, 10% acetonitrile; 0.25 µg/sample) in an automated ProGest Protein Digestion Workstation (Genomic Solution Ltd., Cambridgeshire, UK) following the manufacturer's instructions. Tryptic digests were dried in a SpeedVac (Savant[™], Thermo Scientific Inc., West Palm Beach, FL, USA), redissolved in 15 µL of 0.1% formic acid in water, and submitted to LC-MS/MS. To this end, tryptic peptides were separated by nano-Acquity UltraPerformance LC[®] (UPLC[®]) using BEH130 C18 (100 µm × 100 mm, 1.7 µm particle size) column in-line with a SYNAPT[®] G2 High Definition Mass Spectrometry System (Waters Corp. Milford Massachusetts, USA), run under the same chromatographic conditions as above. Doubly, triply and quadruply charged ions were selected for collision-induced dissociation (CID) MS/MS. Fragmentation spectra were interpreted (a) manually (*de novo* sequencing); (b) using the on-line form of the MASCOT program at <http://www.matrixscience.com> against the NCBI non-redundant database; and (c) processed in Waters Corporation's ProteinLynx Global SERVER 2013 version 2.5.2 (with Expression version 2.0) against the *Aspidelaps scutatus intermedius* venom gland transcriptomic database. MS/MS mass

tolerance was set to ± 0.6 Da. Carbamidomethyl cysteine and oxidation of methionine were selected as fixed and variable modifications, respectively. Amino acid sequence similarity searches were performed against the available databanks using the BLAST program implemented in the WU-BLAST2 search engine at <http://www.bork.embl-heidelberg.de>.

The relative abundances (expressed as percentage of the total venom proteins) of the different protein families were calculated as the ratio of the sum of the areas of the reverse-phase chromatographic peaks containing proteins from the same family to the total area of venom protein peaks in the reverse-phase chromatogram [29, 30]. When more than one protein band was present in a reverse-phase fraction, their proportions were estimated by densitometry of Coomassie-stained SDS-polyacrylamide gels using ImageJ version 1.47 (<http://rsbweb.nih.gov/ij>). Conversely, the relative abundances of different proteins contained in the same SDS-PAGE band were estimated based on the relative ion intensities of the three more abundant peptide ions associated with each protein by MS/MS analysis. Finally, protein family abundances were estimated as the percentages of the total venom proteome.

Immunological assays

1D SDS-PAGE gel electrophoresis and immunoblotting

For one-dimensional (1D) SDS-PAGE gel electrophoresis and immunoblotting we followed our recently described protocol [20, 31]. Briefly, we mixed 10 μ g of each venom with a 1:1 ratio of reduced protein loading buffer, before incubating the samples at 100°C for 10 minutes. The samples were then loaded onto 10-well Mini-PROTEAN TGX precast AnykD gels (Bio-Rad), alongside 5 μ l of protein marker (Broad Range Molecular Marker, Promega), and run at 100 V for 90 minutes using a Mini-PROTEAN Tetra System (Bio-Rad). Resulting proteins gels were: (i) stained with coomassie brilliant blue overnight and then destained (4.5:1:4.5 methanol:acetic acid:H₂O) for visualisation, and (ii) transferred to 0.45 μ m nitrocellulose membranes for immunoblotting experiments using a Trans-Blot Turbo Transfer System (Bio-Rad). For immunoblotting, following confirmation of successful protein transfer by reversible Ponceau S staining, the membranes were incubated overnight in 5% non-fat milk in TBST buffer (0.01 M Tris-HCl, pH 8.5; 0.15 M NaCl; 1% Tween 20) and then washed six times in TBST over 90 mins, before incubation overnight at 4°C with the primary antibodies (SAIMR polyvalent antivenom) diluted 1:5,000 in 5% non-fat milk in TBST. Blots were washed again and incubated for 2 hr at room temperature with rabbit anti-horse horseradish peroxidase-conjugated secondary antibodies (Sigma-Aldrich) diluted

1:2,000 in PBS. After a final TBST wash, immunoblots were visualised with the addition of DAB substrate (50 mg 3,3-diaminobenzidine, 100 ml PBS, 0.024% hydrogen peroxide) for 10 sec.

End-point titration and avidity ELISAs

For end point titration ELISAs, we used our previously described protocols [20, 32]. In brief, 96 well, flat bottomed, ELISA plates (Nunc) were coated with 100 ng of each venom prepared in carbonate buffer, pH 9.6 and the plates incubated at 4°C overnight. Plates were washed after each stage, using six changes of TBST (0.01 M Tris-HCl, pH 8.5; 0.15 M NaCl; 1% Tween 20). Plates were then incubated at room temperature (RT) for 3 hours with 5% non-fat milk (diluted with TBST) to 'block' non-specific reactivity, before washing and incubation with SAIMR polyvalent antivenom overnight at 4°C. The addition of primary antibodies was performed in triplicate with an initial dilution of 1:100 followed by 1:5 serial dilutions. Plates were washed and then incubated in horseradish peroxidase-conjugated rabbit anti-horse IgG (1:2,000; Sigma) for 3 hours at RT. Following washing, the results were visualized by the addition of substrate (0.2% 2,2'-azino-bis (2-ethylbenzthiazoline-6-sulphonic acid) in citrate buffer, pH 4.0 containing 0.015% hydrogen peroxide (Sigma, UK) and optical density (OD) measured at 405nm. The end point titre was defined as the dilution at which the absorbance was greater than that of the baseline plus two standard deviations.

The avidity ELISA was performed as above except that the SAIMR polyvalent antivenom was diluted to a single concentration of 1:12,500, incubated overnight at 4°C, washed with TBST and the chaotrope, ammonium thiocyanate, added to the wells in a range of concentrations (0–8 M) for 15 minutes. Plates were washed, and all subsequent steps were the same as the end point titration ELISA. The relative avidity was determined as the concentration of ammonium thiocyanate required to reduce the control ELISA OD reading (with no chaotrope) by 50%.

Third-generation antivenomics

Third-generation antivenomics [33] was applied to assess the immunoreactivity of the SAIMR antivenom against venom from *A. l. lubricus* and *A. l. cowlesi*. One vial of antivenom was dissolved in 10 mL of the supplied diluent, dialysed against MilliQ® water, lyophilised, and reconstituted in 10 mL of 0.2 M NaHCO₃, 0.5 M NaCl, pH 8.3 (coupling buffer). The concentrations of the antivenom stock solution was determined spectrophotometrically using an extinction coefficient for a 1 mg/mL concentration ($\epsilon^{0.1\%}$) at 280 nm of 1.36 (mg/mL)⁻¹ cm⁻¹ [34]. Antivenom affinity columns were prepared in batch. Three mL of CNBr-activated Sepharose™ 4B matrix (Ge Healthcare,

Buckinghamshire, UK) were packed in a ABT column (Agarose Bead Technologies, Torrejón de Ardoz, Madrid) and washed with 10x matrix volumes of cold 1 mM HCl, followed by two matrix volumes of coupling buffer to adjust the pH to 7.0-8.0. CNBr-activated instead of N-hydroxysuccinimide (NHS)-activated matrix was employed because NHS released during the coupling procedure absorbs strongly at 280 nm, thus interfering with the measurement of the concentration of antibodies remaining in the supernatant of the coupling solution. Forty mg of antivenom was dissolved in 2x matrix volume of coupling buffer and incubated with 3 mL of CNBr-activated matrix for 4 h at room temperature. Antivenom coupling yield, estimated measuring $A_{280\text{nm}}$ before and after incubation with the matrix, was 19.9 mg/mL. After the coupling, remaining active matrix groups were blocked with 12 mL of 0.1 M Tris-HCl, pH 8.5 at room temperature for 4 h. Affinity columns, each containing 352 μL (7.0 mg) of immobilised antivenom, were alternately washed with three matrix volumes of 0.1 M acetate containing 0.5 M NaCl, pH 4.0-5.0, and three matrix volumes of 0.1 M Tris-HCl, pH 8.5. This procedure was repeated 6 times. The columns were then equilibrated with 5 volumes of working buffer (PBS, 20 mM phosphate buffer, 135 mM NaCl, pH 7.4) and incubated with increasing amounts (100-1200 μg of total venom proteins) of venom dissolved in $\frac{1}{2}$ matrix volume of PBS, and the mixtures incubated for 1 h at 25 °C in an orbital shaker. As specificity controls, 350 μL CNBr-activated Sepharose™ 4B matrix, without (mock) or with 7 mg of immobilised control (naïve) horse IgGs, were incubated with venom and developed in parallel to the immunoaffinity columns. The non-retained eluates of columns incubated with 100-600 μg and 900-1200 μg venom were recovered with 5x and 10x matrix volume of PBS, respectively, and the immunocaptured proteins were eluted, respectively, with 5x and 10x matrix volume of 0.1M glycine-HCl, pH 2.7 buffer and brought to neutral pH with 1M Tris-HCl, pH 9.0. The entire fractions eluted with 5x and $\frac{1}{2}$ of the fractions recovered in 10x matrix volume were concentrated in a Savant SpeedVac™ vacuum centrifuge (ThermoFisher Scientific, Waltham, MA USA) to 40 μL , and aliquots corresponding to 150 initial total venom proteins were fractionated by reverse-phase HPLC using an Agilent LC 1100 High Pressure Gradient System (Santa Clara, CA, USA) equipped with a Discovery® BIO Wide Pore C18 (15 cm x 2.1 mm, 3 μm particle size, 300 Å pore size) column and a DAD detector as above. Eluate was monitored at 215 nm with a reference wavelength of 400 nm. The fraction of non-immunocaptured molecules was estimated as the relative ratio of the chromatographic areas of the toxin recovered in the non-retained (NR) and retained (R) affinity chromatography fractions using the equation

$$\%NR_i = 100 - [(R_i / (R_i + NR_i)) \times 100],$$

where R_i corresponds to the area of the same protein "i" in the chromatogram of the fraction retained and eluted from the affinity column.

Toxicity and neutralisation assays

All *in vivo* animal experimentation was conducted using protocols approved by the Animal Welfare and Ethical Review Boards of the Liverpool School of Tropical Medicine and the University of Liverpool, and performed in specific pathogen free conditions under licenced approval (PPL4003718) of the UK Home Office, in accordance with the Animal [Scientific Procedures] Act 1986 and institutional guidance on animal care. Experimental design was based upon refined WHO-recommended protocols [20, 32, 35, 36].

***In vivo* venom toxicity**

We determined the median lethal dose (venom LD_{50}) of *A. s. intermedius* and *N. nivea* venom, using the previously described method [20, 32]. Briefly, groups of five male 18-22g CD-1 mice (Charles River, UK) received varying doses of each venom in 100 μ l PBS via intravenous (tail vein) injection, and after 7 hr surviving animals were recorded. Animals were continuously monitored for the duration of the experiment and euthanised upon observation of humane endpoints (e.g. external signs of haemorrhage, seizure, pulmonary distress, paralysis). The amount of venom that causes lethality in 50% of the injected mice (the LD_{50}) and the 95% confidence intervals were calculated using probit analysis [37]. Due to limited venom supplies, and also to reduce experimental animal numbers, we only performed limited range-finding venom toxicity studies with the other *Aspidelaps* venoms. We tested the toxicity of *A. l. lubricus* venom at four different doses, each in a single experimental animal, while *A. l. cowlesi* venom was delivered to two mice at a single dose of 5 μ g. Euthanised animals from the experiments described above were subjected to post-mortem macroscopic examination, with gross pathology recorded.

***In vivo* venom neutralisation**

To assess the efficacy of the SAIMR polyvalent antivenom at neutralising the lethal effects of *Aspidelaps* venom we used the median effective dose (ED_{50}) assay; a WHO-recommended test for determining the least amount of antivenom required to prevent death in 50% of mice injected with lethal doses of venom [36, 38]. Using a previously described protocol [20, 32], various doses of the SAIMR polyvalent antivenom were mixed with 2 x LD_{50} s of *A. s. intermedius* (2 x LD_{50} = 11.5 μ g) or *N. nivea* venom (2 x LD_{50} = 30.1 μ g) in 200 μ l PBS, and the mixture incubated at 37°C for 30 minutes. As described above, the mixture was then intravenously injected into the tail vein of

groups of five male 18-22g CD-1 mice and after 7 hr the surviving animals were recorded. The median effective dose (ED_{50}) and 95% confidence limits were calculated using probit analysis [37].

RESULTS AND DISCUSSION

The *Aspidelaps scutatus intermedius* venom gland transcriptome

Sequencing of the *A. s. intermedius* venom gland transcriptome resulted in 2,523 assembled contigs. Using BLAST annotations, we classified these contigs into three categories: those encoding toxin families previously described in the literature, those encoding non-toxin 'housekeeping' genes, and those with no significant BLAST hit. Consistent with other previously described snake venom gland transcriptomes [39-44], toxin encoding contigs accounted for the majority of gene expression observed (54.6%, Fig. 1), despite being represented by a small proportion of the contigs (66 contigs, 3.3% of total contig numbers). In contrast, we recovered 1,783 contigs encoding non-toxins, which represented 41.6% of total transcriptome expression, and a total of 674 contigs (4.0% of total expression) that exhibited no significant hit to sequences in the NCBI NR database (Fig. 1).

In line with previous venom gland transcriptomic studies on elapid snakes [22, 42, 45], we observed considerable toxin gene complexity. A total of 17 different toxin-encoding gene families were identified (Fig. 1, Supplementary Table S1), although only five of these, three-finger toxin (3FTx), phospholipase A₂ (PLA₂), Kunitz-type inhibitor (KUN), cysteine-rich secretory protein (CRISP) and C-type natriuretic peptides precursor (C-NP prec) exhibited expression levels of >1% of all toxin encoding mRNAs, and only two (3FTx and PLA₂) exhibited total toxin transcript expression levels of >3% (Fig. 1, Supplementary Table S1). 3FTxs were the dominant toxin-coding transcript type recovered, both in expression level (65.3% of total toxin mRNAs) and number of family members, with 27 unique contigs encoding 23 different (19 full-length) 3FTx proteins (Table S1). BLAST-based structural annotations included cytotoxins (CTxs), aminergic (muscarinic) toxins (MTxs), type I (short) and type II (long) neurotoxins (NTxs), weak toxins (WTxs) and a pre-synaptic buccandin-like neurotoxin. CTx S₄C₈ and two isoforms of CTx S₃C₂ (Joubert, 1988c), each representing 22-24% of total toxin transcripts expression (12-13% of the total venom gland transcriptome), were the most abundant 3FTx-coding mRNAs (Fig. 1, Table S1).

The second most abundant gene family expressed in the venom gland transcriptome of *A. s. intermedius* was PLA₂. This toxin transcript class represented 23.8% of total toxin transcripts expression (13% of the total venom gland

transcriptome), which encoded 1-2 putative isocontigs (e.g. contigs differing in a single nucleotide) for the group IA acidic PLA₂ CM-II [P07037] [15] (Fig. 1, Table S1). Whether these single nucleotide variants mirror the existence of two highly similar gene products or results from a sequencing error remains obscure. The remaining 14 venom toxin transcript families exhibited lower expression levels, with each representing less than 3% of the total abundance of toxin encoding contigs and, in combination, representing <11% of all toxin-coding mRNAs (Fig. 1, Table S1). Amongst these lowly expressed genes, the four KUN contigs accounted for 2.54% of all toxin transcripts, making it the third most abundant toxin gene family. Contigs T0353, T0399 and T1458 encoded single Kunitz-domains and, in combination, dominate the KUN expression detected (2.51%). Contig T0053 encoded two tandemly arranged Kunitz domains exhibiting sequence similarity with the unusual two-domain Kunitz-type proteinase inhibitor reported from the South Australian Kangaroo Island endemic pygmy copperhead (*Austrelaps labialis*) venom gland [46]. All remaining putative toxin transcript types identified in the *A. s. intermedius* venom gland transcriptome were found expressed at very low levels (<1.4% of the total toxin encoding genes) and included: six SVMP contigs, four C-NP precursor contigs, and single contigs encoding full-length cysteine-rich secretory protein (CRISP), nawaprin (NAW), cobra venom factor (CVF), phospholipase B (PLB), phosphodiesterase (PDE), vespryn, snake venom serine protease (SVSP), nerve growth factor (NGF), L-amino acid oxidase, dipeptidyl peptidase IV (DPP IV), 5'-nucleotidase (5'-NT), and hyaluronidase (HYAL) (Fig. 1, Table S1). Altogether the transcriptomic dataset consists of 66 contigs merged into 51-53 toxin-coding mRNAs, of which 41 include full-length toxin sequences (Table S1).

The divergent venom proteomes of A. s. intermedius and A. lubricus subspecies

The venom proteomes of adult *A. s. intermedius*, *A. l. lubricus*, and *A. l. cowlesi* specimens were characterized and quantified applying the previously described [29, 30] two-step pre-MS decomplexation protocol (reverse-phase HPLC and SDS-PAGE) (Fig. 2, panels A, C and E), followed by peptide-centric bottom-up, transcriptome-aided MS/MS analysis of tryptic digests from SDS-PAGE separated protein bands eluted in the different RP chromatographic fractions [47].

Comparative proteomics analysis revealed a high degree of conservation of the global composition of the three *Aspidelaps* venom proteomes (Fig. 2), all characterized by the overwhelming predominance of 3FTxs (76-83% of the total venom toxins). All three venoms shared modest to moderate relative abundance of KUN (1-9%), PLA₂ (5-6%), CRISP (3.5-5%), PIII-SVMP (3-5%), and PDE (0.4-1%). svNGF was found in *A. s.*

intermedius (1.7%) and *A. I. lubricus* (0.1%) (Fig. 2 panels B and D, respectively), whereas LAO was equally (1%) present in both subspecies of *A. lubricus* (Fig. 2, panels D and F, respectively), and a low amount of HYAL (0.1%) was uniquely identified in the venom of *A. I. cowlesi* (Fig. 2, panel F). Supplementary Tables S2-S4 provide details of the assignment, quantification, and matching to the transcriptomic database of the RP-HPLC separated venom proteins of *A. s. intermedius*, *A. I. lubricus*, and *A. I. cowlesi*, respectively. Isotope-averaged masses of intact *A. I. cowlesi* toxins were also recorded by ESI LC-MS (Supplementary Table S4).

Proteomic hits were predominately matched to transcriptome contigs and the closest homolog toxin present in the NCBI database was identified by BLAST analysis. The picture that emerged when the relative abundances of the different 3FTx classes were mapped on the species' pie charts revealed distinct compositional patterns for *A. s. intermedius* on the one hand and the *A. lubricus* subspecies on the other. Thus, whereas the venom proteome of *A. s. intermedius* is mostly composed of cytotoxins (S_4C_8 and S_3C_2 , 33.7%) and post-synaptic α -neurotoxins of type I (short α -NTx-1 and atratoxin b [*N. annulifera* P68417]-like, 12.5%) and type II (long-chain NTx-1 S_4C_6 and α -NTx, 31.2%) (Fig. 2B), the venoms from both *A. lubricus* subspecies contain lower proportion of cytotoxins (S_3C_2 , 2-5%; S_4C_8 , absent) and higher concentrations (22-26%) of α -neurotoxin(s) homologous to the Chinese cobra *N. atra* atratoxin b [AAR33036] and long-chain NTx-1 S_4C_6 (40-42%) (Fig. 2, panels D and F). In addition, a weak neurotoxin (homolog of *N. haje* wNTx CM-II, 1.8%) identified in the venom of *A. s. intermedius* was absent from the *A. lubricus* venoms, which, in turn, present non-conventional (nc) 3FTxs (2-3%) similar to *Bungarus flaviceps* ADF50020, and a pre-synaptic neurotoxic 3FTx (β -NTx, 1-2%) homolog of *B. candidus* bucandin [P81782], which was not found in the venom of *A. s. intermedius*.

Comparison of the toxin composition of *A. s. intermedius* venom gland transcriptome and venom proteome revealed both qualitative and quantitative differences. Thus, several putative toxin families observed in the transcriptome were not detected in the venom proteome (Fig. 1). On the other hand, the major discrepancies between gene expression and proteomic abundance correspond to the 3FTx class, which experience a net increase of 15.2%, while the acidic PLA₂ CM-II [P07037], decreased by 17.7% (Table 1). Among the 3FTxs, the change of expression is disparate. While long NTx-1 S_4C_8 increased its relative abundance by 10-fold (T, 2.8%; P, 28.9%), the relative abundance of CTx S_3C_2 decreased from 23.8% (T) to 10.5% (P), whereas the level of expression of CTx S_4C_8 remained constant (T = P, 22%) (Table 1). These major changes between gene expression and proteomic

abundance may result from post-transcriptional modulation of mRNA translation [48-50], although further studies are needed to address this issue.

The *Aspidelaps* venom proteomes, dominated by cytotoxic and/or neurotoxic 3FTxs, seemingly account for the reported neurological (*A. l. lubricus*) and cytotoxic (*A. s. scutatus*) manifestations of the few documented *Aspidelaps* snakebite envenomings described from humans [4-9], and from experimental studies in mice [5]. To delve into the mechanism of action underpinning lethality by *Aspidelaps* venom we determined the toxicity of *Aspidelaps* venom *in vivo*, and performed behavioural observations of envenomed mice and assessments of post-mortem pathology.

Toxicity and toxicovenomics of *Aspidelaps* venoms

To determine the toxicity of *Aspidelaps* venom *in vivo*, we intravenously (i.v.) injected groups of mice with varying doses of *A. s. intermedius* venom. The i.v. murine lethal dose 50 (LD₅₀) of *A. s. intermedius* venom was found to be 5.75 µg/mouse (5.29–6.26 µg, 95% CI [0.2875 mg/kg]), which is more potent than that obtained with *N. nivea* venom (15.05 µg/mouse [10.20–18.70 95% CI]; 0.7525 mg/kg). Consequently, the murine toxicity of *A. s. intermedius* venom is highly comparable with some of the most toxic, medically important, elapid snakes of sub-Saharan Africa (e.g. *D. polylepis* 6.17 µg/mouse; *N. haje* 8.15 µg/mouse; *N. pallida* 9.29 µg/mouse; [20, 22]). Limited range-finding toxicity experiments with venom from *A. l. lubricus* suggested a comparable LD₅₀ with than of *A. s. intermedius* (four mice tested at different doses; survival at 2 µg/mouse and death at ≥5 µg/mouse). Equivalent experiments with *A. l. cowlesi* venom were inconclusive due to insufficient venom - two mice were tested and both survived a dose of 5 µg. Nevertheless, the data suggested a lower toxicity than its congeners in the murine model.

Taking advantage of the availability of LD₅₀ values for the major individual toxins and 3FTx subfamilies identified in the *Aspidelaps* venoms (Fig. 2), we applied a toxicovenomics approach to calculate theoretical LD50s for the three *Aspidelaps* venoms (Table 2). To this end, the contribution of a given toxin "i" to the venom's LD₅₀ was calculated as

$$fLD_{50} \text{ Toxin}_i = (\% \text{Toxin}_i) \times (LD_{50} \text{ Toxin}_i)$$

The combined contribution of toxins other than 3FTxs and PLA₂ (eg, "other Txs" = KUN, CRISP, PIII-SVMP, PDE, LAO, HYAL and vNGF) was estimated for *A. s. intermedius* as 20 µg/g mouse using the equation:

$$fLD_{50} \text{ "otherTxs"} = (\text{Experimental LD}_{50} \text{ Asi} - \sum fLD_{50} \text{ Toxin}_i) / (\% \text{ "otherTxs"})$$

This value was used in the calculations of the theoretical LD₅₀s for *A. l. lubricus* and *A. l. cowlesi* venoms, resulting in 4.12-6.45 µg/g and 4.18-5.75 µg/g, respectively (Table 2). The good correspondence between these theoretical values and those determined on the basis of partial experimental data suggests that synergies between different toxins may not play a significant role in the toxicity of *Aspidelaps* venoms, as has been shown for other venoms [51-53].

Pathological effects induced by A. s. intermedius venom

To assess the mechanism of action underpinning lethality by *Aspidelaps* venom, we performed (i) behavioural observations of envenomed mice and (ii) assessments of post-mortem pathology. At doses of 5-7 µg of *A. s. intermedius* venom all mice exhibited classical signs of systemic neurotoxicity with respiratory paralysis, characterised by ataxia, slumping and dyspnoea. Neurologically, this behaviour is consistent with blockade of neuromuscular transmission by either inhibition of binding to cholinergic receptor or damage to the presynaptic nerve terminal. Sixty minutes after administration of the 7 µg venom dose, all of the mice were euthanised on ethical grounds. Post-mortem analysis of mice i.v. injected with 6 µg and 7 µg of *A. s. intermedius* venom revealed the collapse of both lungs (n=6). Without further analysis, it is not possible to determine which of the toxins is responsible for the observed neurotoxicity. However, given the notable abundance of both type I and II post-synaptic 3FTx neurotoxins detected in the venom, which are capable of targeting both neuromuscular and neuronal nicotinic acetylcholine receptors [54, 55], it seems reasonable to assume that these toxins are at least partially responsible.

All experimental animals also exhibited evidence of haemorrhage into the atria (n=6), with seemingly selective sub-epicardial haemorrhage of the right ventricle (no abnormality was detected in the left ventricle) in the majority (4/6) of mice. Furthermore, incoagulable blood was observed in 3/6 mice, haemoperitoneum (blood within the peritoneal cavity) observed for 2/6 mice, and substantial haemothorax (free blood in chest cavity) observed in one mouse; suggesting that in addition to neurotoxic venom toxins, a notable cardiotoxic and haemotoxic component exists in the venom of *A. s. intermedius*. No obvious abnormalities were observed in the intestines, spleen, stomach, kidneys or brain, but haemorrhage was observed in the membranes surrounding the brain.

Proteins of the 3FTx family are amongst the most functionally diverse groups of snake venom toxins, exhibiting a wide variety of pharmacological effects including neurotoxic, cytotoxic, cardiotoxic, anticoagulant, and antiplatelet activities [55, 56].

Cardiotoxic 3FTxs exert their toxicity by forming pores in cell membranes [57], and both cardiotoxic and anticoagulant PLA₂ molecules have been also characterized in snake venoms [52, 58]. Future toxicovenomic analysis of the cytotoxins S₂C₃ and S₄C₈ and the PLA₂ CM-II should reveal the pathophysiological relevance of these toxins in the cardiotoxic and haemotoxic effects produced by the administration of *A. s. intermedius* venom.

Immunological cross-reactivity of *Aspidelaps* venoms with SAIMR polyvalent antivenom

Antivenom is the treatment of choice for the neurotoxic and haemotoxic effects of systemic snake envenoming, and its efficacy is generally considered to be predominately restricted to the snakes whose venom was used in its manufacture or, in some cases, their congeners [1, 32, 59-62]. No commercial antivenom is made using venom from species of the genus *Aspidelaps*. The South African Vaccine Producers "SAIMR polyvalent" antivenom is generated by immunising horses with the venoms of related African species of Elapidae [63], including species from the genera *Naja* (*Naja nivea*, *N. melanoleuca*, *N. annulifera* and *N. mossambica*), *Hemachatus* (*Hemachatus haemachatus*), and *Dendroaspis* (*D. angusticeps*, *D. jamesoni*, and *D. polylepis*), and species of the genus *Bitis* (*B. arietans* and *B. gabonica*) of the Viperidae family. This antivenom is commonly available throughout the southern regions of Africa where *Aspidelaps* spp. are distributed [11]. For these reasons, we screened the immunological cross-reactivity of the SAIMR polyvalent antivenom with venoms from *A. s. intermedius*, *A. l. lubricus* and *A. l. cowlesi*, and used venom from the neurotoxic cobra *N. nivea* as a comparator.

We first performed immunoblotting experiments to visualise the antivenom antibody (equine F(ab')₂) cross-reactivity with the proteins of the three *Aspidelaps* venoms, and that of *N. nivea* (Fig. 3A). The SAIMR polyvalent antivenom exhibited extensive recognition of the various *Aspidelaps* venom toxins, in a comparable inter-specific manner. Extensive binding was observed to the abundant lower molecular weight proteins (3FTxs and PLA₂), and to less abundant toxins of higher molecular weights. As anticipated, the intensity of antibody-protein bands was greatest in the *N. nivea* venom used for comparison.

We next used ELISA experiments to quantitate the amount of binding (end-point titration ELISA) and the strength of binding (avidity ELISA). The end-point ELISA results demonstrated substantial decreases in binding from the positive control (*N. nivea* venom) to the three *Aspidelaps* spp. (Fig. 3B). Nonetheless, the antibody-venom protein binding levels were substantially higher than the baseline, demonstrating that

the SAIMR polyvalent antivenom recognises and binds extensively to *Aspidelaps* venom toxins. The end-point dilution titres observed for the three *Aspidelaps* venoms were identical (all were 1:62,500), and are therefore comparable to prior studies describing interactions between African snake venoms and polyvalent antivenoms [20], but, as anticipated, are lower than when using monospecific antivenoms and homologous venoms [32]. Although there were no quantitative differences in the end-point dilutions observed between the three *Aspidelaps* species, the level of binding observed with *A. s. intermedius* venom at lower dilutions was noticeably higher than that of its two congeners (Fig. 3B). Contrastingly, the relative avidity ELISA revealed little difference in the strength of antibody binding observed between the venoms of *N. nivea*, *A. l. lubricus* and *A. l. cowlesi* (Fig. 3C). The concentration of the chaotropic agent (ammonium thiocyanate) required to reduce ELISA readings by 50% was the same for all three species (6M), although, in contrast with the end-point ELISA, it was noticeably lower for *A. s. intermedius* (4M) (Fig. 3C) – suggesting that the degree of venom variation observed between this species and its congeners (Fig. 2) may result in weaker antibody interactions with the SAIMR polyvalent antivenom. Despite this, 50% reductions in binding in the presence of 4M ammonium thiocyanate is highly comparable with prior studies using SAIMR polyvalent antivenom and various snake venoms that this product neutralises *in vivo* [20].

Antivenomics analysis of the preclinical efficacy of SAIMR antivenom toward *Aspidelaps* venom

The toxin recognition landscape of SAIMR antivenom was also assessed using third-generation antivenomics [33]. Analysis of the concentration-dependent immunocapturing profile of SAIMR antivenom affinity columns toward the venom toxins of *A. l. cowlesi* (Fig. 4A, Table 3A) and *A. l. lubricus* (Fig. 4B, Table 3B) showed paraspecific immunoreactivity against all the *Aspidelaps* toxin classes. The maximal binding capacity of immobilised (7 mg) SAIMR F(ab')₂ antibodies was 80.45 µg and 98.64 µg of *A. l. cowlesi* and *A. l. lubricus* venom toxins respectively, which correspond to maximum capacities per vial (10 mL, 118.4 mg F(ab')₂/mL) of 13.60 mg and 14.09 mg of venom. It is worth noting that 41% (*A. l. cowlesi*) and 49% (*A. l. lubricus*) of the SAIMR antivenom's ability to bind *Aspidelaps* toxins corresponds to anti-3FTx antibodies. For a calculated average molecular mass of 10.6 kDa for the various venom proteins, these antivenomics results suggest that 5.9% and 7.3% of the SAIMR antibodies recognize toxins from *A. l. cowlesi* and *A. l. lubricus*, respectively. These figures fall within the low range of percentages of anti-toxin antibodies (4-24%) determined, however, in a yet still small number of commercial antivenoms (JJC,

unpublished results).

In vivo neutralisation of Aspidelaps venom lethality by SAIMR polyvalent antivenom

We next sought to assess whether the promising immunological cross-reactivity observed between the SAIMR polyvalent antivenom and *Aspidelaps* venoms (Figs. 3 and 4, Table 3) would translate into the murine preclinical neutralisation of venom-induced lethality *in vivo*. To this end, we performed median effective dose 50 (ED₅₀) assays [35, 36] using *A. s. intermedius* venom and the SAIMR polyvalent antivenom, and compared these results with those obtained using venom from *Naja nivea*. For both experiments the mice were challenged with 2 LD₅₀s of each venom. The SAIMR polyvalent antivenom effectively neutralised the lethal effects of both venoms, although it was more efficacious at lower doses against *N. nivea* venom. The ED₅₀s against *A. s. intermedius* and *N. nivea* venoms were 24.52 µl antivenom per mouse [21.45-27.65 µl, 95% CI] and 15.95 µl [13.96-18.23 µl, 95% CI], respectively. The neutralising potency of the SAIMR antivenom (P, in milligrams of venom neutralized by 1 mL of antivenom), calculated as $P = [(T_v - 1)/DE_{50}] \times LD_{50}$, where T_v is the number of LD₅₀s [mg V/mouse] in the test dose of venom, and ED₅₀ is the median effective dose of the antivenom in ml/mouse [64], was 0.235 mg venom/mL antivenom (*A. s. intermedius*) and 0.944 mg venom/mL antivenom (*N. nivea*).

The percentage of antibodies that recognise *Aspidelaps* toxins and contribute to the lethality neutralising capacity of lethality of SAIMR antivenom can be calculated by the equation %neutralising F(ab')₂ = (P/maximal venom binding capacity). Assuming that SAIMR potency against *A. l. cowlesi* and *A. l. lubricus* venoms lethality does not strongly depart from that determined for *A. s. intermedius*, 17.3% and 13.8% of *A. l. cowlesi* and *A. l. lubricus* toxin-recognising F(ab')₂ molecules may also bear lethality neutralising activity. These findings strongly suggest that, although the SAIMR antivenom is four times less effective at neutralising *A. s. intermedius* venom than that of *N. nivea*, in the current absence of any *Aspidelaps*-specific antivenom, this polyvalent antivenom could be a useful therapeutic tool for treating human envenomings by *Aspidelaps* species. These findings will, however, require future clinical validation.

CONCLUDING REMARKS

Our results demonstrate that snakes of the genus *Aspidelaps* have venom abundant in 3FTx and PLA₂ toxins, but that *A. s. intermedius* and the *A. lubricus* subspecies

lubricus and *cowlesi* differ in terms of the abundance of 3FTx isoforms found in their venom. Despite these snakes having much smaller venom yields than many other African elapid snakes (e.g. mambas [*Dendroapsis* spp.] and cobras [*Naja* spp.]), due to their much smaller size, we demonstrate that members of this genus have highly toxic venom, whose effects are characterised by systemic neurotoxicity resulting in respiratory paralysis and notable cardiotoxic and haemotoxic pathologies in a murine model of envenoming. These findings correlate with the limited clinical information available relating to bites by *Aspidelaps*, and highlight that the toxicity of *Aspidelaps* venoms, on a weight by weight basis, is equivalent to that of cobras and mambas. However, the considerably higher venom volumes of the latter suggest that human systemic envenoming by *Aspidelaps* species may not be as life-threatening as that from cobras and mambas. We also demonstrate that the SAIMR polyspecific antivenom exhibits pre-clinical neutralising capability against the venom of *A. s. intermedius*, and probably also against the venoms of the *A. lubricus* subspecies. Thus, we recommend that this antivenom be trialled for its use in treating systemic envenoming by *Aspidelaps* snake species.

ACKNOWLEDGMENTS

The authors wish to thank Paul Rowley and John Dunbar for expert maintenance of the *Aspidelaps* spp. used in this study and for the collection of venom. This project was funded by a UK Medical Research Council Research Grant (MR/L01839X/1) to RAH, NRC, J-MG and JJC, and grant BFU2013-42833-P (Ministerio de Economía y Competitividad, Madrid, Spain) to JJC.

AUTHOR CONTRIBUTIONS

RAH, GW, NRC and JJC devised the project concept; GW, NRC, RAEL and SCW performed transcriptomic experiments; DP, SQ-B and JJC performed venom and antivenomic experiments, GW and RAH undertook immunological analyses; NRC, FMSB, J-MG and RAH performed toxicity and neutralisation experiments; GW, NRC, JJC and RAH wrote the paper.

REFERENCES

- [1] J.M. Gutiérrez, J.J. Calvete, A.G. Habib, R.A. Harrison, D.J. Williams, D.A. Warrell, Snakebite envenoming. *Nat. Rev. Dis. Primers* 3 (2017) 17079.
- [2] WHO 2010. WHO Regional Office for Africa. Guidelines for the prevention and clinical management of snakebite in Africa. <http://apps.who.int/medicinedocs/en/d/Js17810en/>.
- [3] J. Visser, D.S. Chapman, Snakes and Snakebite. *Venomous Snakes and Management of Snakebite in Southern Africa*. Purnell, Cape Town, South Africa, (1978). ISBN: 1-86872-933-8.
- [4] W.R. Branch, The venomous snakes of southern Africa Part 2. *Elapidae* and *Hydrophidae*. *The Snake* 11 (1979) 199-225.
- [5] S. Spawls, B. Branch, The dangerous snakes of Africa: natural history, species directory, venoms, and snakebite. Ralph Curtis Publishing, Sanibel Island, FL, (1995). ISBN 978-0-88359-029-4.
- [6] K.C. van Egmond, A fatal bite by the shield-nose snake (*Aspidelaps scutatus*). *S. Afr. Med. J.* 66 (1984) 714.
- [7] M. Zaltzman M. Rumbak, M. Rabie, S. Zwi, Neurotoxicity due to the bite of the shield-nose snake (*Aspidelaps scutatus*): a case report. *South African Medical Journal* 66 (1984) 111-112.
- [8] G.V. Haagner G. Carpenter, Venoms and snakebite: *Aspidelaps s. scutatus* shield-nosed snake, envenomation. *Journal of the Herpetological Association of Africa* 37 (1990) 37, 60.
- [9] T. Ulber, Erfahrungen mit dem Biß der Korallenkobra *Aspidelaps lubricus lubricus* (Laurenti, 1768) (Serpentes: Elapidae). *Sauria* 20 (1998) 33-36.
- [10] D.G. Broadley, Fitzsimons' snakes of Southern Africa. In *Family Elapidae Cobras, Mambas, Coral and Garter-Snakes etc.*, Delta Books (Pty) Ltd, Johannesburg, (1983) 267-302. ISBN 13: 9780908387045.
- [11] D.G. Broadley, A.S. Baldwin, Taxonomy, natural history, and zoogeography of the Southern African Shield Cobras, genus *Aspidelaps* (Serpentes: Elapidae). *Herpetological Natural History* 9 (2006) 163-176.
- [12] A. Deufel, Burrowing with a kinetic snout in a snake (Elapidae: *Aspidelaps scutatus*). *J. Morphology* 278 (2017) 1706-1715.
- [13] J.A. Marais, Complete guide to the snakes of Southern Africa. Southern Book Publishers (Pty) Ltd, Johannesburg (1992).
- [14] P.A. Christensen, The venoms of central and south African snakes. *Venomous Animals and Their Venoms vol.1: Venomous Vertebrates* (W. Bücherl, E.E.

- Buckley, V. Deulofeu, eds.), Academic Press, New York, USA, chapter 16 (1968), 437-461. ISBN: 9781483263632.
- [15] F.J. Joubert, Purification, some properties of two phospholipases A₂ (CM-I and CM-II) and the amino-acid sequence of CM-II from *Aspidelaps scutatus* (shield or shield-nose) venom. *Biol. Chem. Hoppe Seyler* 368 (1987) 1597-1602.
- [16] F.J. Joubert, Purification and some properties of low-molecular-weight proteins of *Aspidelaps scutatus* (shield or shield-nose snake) venom. *Int. J. Biochem.* 20 (1988) 49-53.
- [17] F.J. Joubert, Snake venom toxins. I. The primary structure of a long neurotoxin S₄C₆ from *Aspidelaps scutatus* (shield or shield-nose snake) venom. *Int. J. Biochem.* 20 (1988) 93-96.
- [18] F.J. Joubert, Snake venom toxins. II. The primary structures of cytotoxin homologues S₃C₂ and S₄C₈ from *Aspidelaps scutatus* (shield or shield-nose snake) venom. *Int. J. Biochem.* 20 (1988) 337-345.
- [19] W.R. Branch, Venom of the south west African coral snake *Aspidelaps lubricus infuscatus* Mertens. *J. Herpetol. Association Africa* 25 (1981) 2-4.
- [20] R.A. Harrison, G.O. Oluoch, S. Ainsworth, J. Alsolaiss, F. Bolton, A.S. Arias, J.M. Gutiérrez, P. Rowley, S. Kalya, H. Ozwara, N.R. Casewell, Preclinical antivenom-efficacy testing reveals potentially disturbing deficiencies of snakebite treatment capability in East Africa. *PLoS Negl. Trop. Dis.* 11 (2017) e0005969.
- [21] S.A.Jr. Minton, M.R. Minton, *Venomous reptiles*. George Allen and Unwin, London, (1971).
- [22] S. Ainsworth, D. Petras, M. Engmark, R.D. Süßmuth, G. Whiteley, L.O. Albulescu, T.D. Kazandjian, S.C. Wagstaff, P. Rowley, W. Wüster, P.C. Dorrestein, A.S. Arias, J.M. Gutiérrez, R.A. Harrison, N.R. Casewell, J.J. Calvete, The medical threat of mamba envenoming in sub-Saharan Africa revealed by genus-wide analysis of venom composition, toxicity and antivenomics profiling of available antivenoms. *J. Proteomics* 172 (2018) 173–189.
- [23] D. Pla, L. Sanz, G. Whiteley, S.C. Wagstaff, R.A. Harrison, N.R. Casewell, J.J. Calvete, What killed Karl Patterson Schmidt? Combined venom gland transcriptomic, venomomic and antivenomic analysis of the South African green tree snake (the boomslang), *Dispholidus typus*. *Biochim. Biophys. Acta - Gen. Subj.* 1861 (2017) 814-823.
- [24] A. Schroeder, O. Mueller, S. Stocker, R. Salowsky, M. Leiber, M. Gassmann, S. Lightfoot, W. Menzel, M. Granzow, T. Ragg, The RIN: an RNA integrity number for assigning integrity values to RNA measurements. *BMC Mol. Biol.* 7 (2006) 3.

- [25] K. Baumann, N.R. Casewell, S.A. Ali, T.N.W. Jackson, I. Vetter, J.S. Dobson, S.C. Cutmore, A. Nouwens, V. Lavergne, B.G. Fry, A ray of venom: Combined proteomic and transcriptomic investigation of fish venom composition using barb tissue from the blue-spotted stingray (*Neotrygon kuhlii*). *J. Proteomics* 109 (2014) 188–198.
- [26] N.R. Casewell, J.C. Visser, K. Baumann, J. Dobson, H. Han, S. Kuruppu, M. Morgan, A. Romilio, V. Weisbecker, S.A. Ali, J. Debono, I. Koludarov, I. Que, G.C. Bird, G. Cooke, A. Nouwens, W.C. Hodgson, S.C. Wagstaff, K.L. Cheney, I. Vetter, L. van der Weerd, M.K. Richardson, B.G. Fry, The Evolution of Fangs, Venom, and Mimicry Systems in Blenny Fishes. *Curr. Biol.* 27 (2017) 1184–1191.
- [27] J. Archer, G. Whiteley, N.R. Casewell, R.A. Harrison, S.C. Wagstaff, VTBuilder: A tool for the assembly of multi isoform transcriptomes. *BMC Bioinformatics* 15 (2014) 389.
- [28] A. Conesa, S. Götz, J.M. García-Gómez, J. Terol, M. Talón, M. Robles, Blast2GO: a universal tool for annotation, visualization and analysis in functional genomics research. *Bioinformatics* 21 (2005) 3674–3676.
- [29] J.J. Calvete, Next-generation snake venomomics: protein-locus resolution through venom proteome decomplexation. *Expert Rev. Proteomics* 11 (2014) 315–329.
- [30] S. Eichberg, L. Sanz, J.J. Calvete, D. Pla, Constructing comprehensive venom proteome reference maps for integrative venomomics. *Expert Rev. Proteomics* 12 (2015) 557–573.
- [31] S. Ainsworth, J. Slagboom, N. Alomran, D. Pla, Y. Alhamdi, S. King, F. Bolton, J.M. Gutiérrez, F. Vonk, C.H. Toh, J.J. Calvete, J. Kool, R.A. Harrison, N.R. Casewell, The paraspecific neutralisation of snake venom induced coagulopathy by antivenoms. *Commun. Biol.* 1 (2018), 34.
- [32] N.R. Casewell, D.A.N. Cook, S.C. Wagstaff, A. Nasidi, D. Durfa, W. Wüster, R.A. Harrison, Pre-clinical assays predict pan-African *Echis viper* efficacy for a species-specific antivenom. *PLoS Negl. Trop. Dis.* 4 (2010) e851.
- [33] D. Pla, Y. Rodríguez, J.J. Calvete, Third generation antivenomics: pushing the limits of the in vitro preclinical assessment of antivenoms. *Toxins* 9 (2017) E158.
- [34] G.C. Howard, M.R. Kaser, *Making and Using Antibodies: A Practical Handbook*, Second Edition, CRC Press, Taylor & Francis Group, Boca Raton (FL) (2014) 458 pp. ISBN 9781439869086.
- [35] R.D. Theakston, H.A. Reid, H.A. Development of simple standard assay procedures for the characterization of snake venom. *Bull. World Health Organ.* 61 (1983) 949–956.

- [36] World Health Organization. WHO guidelines for the production, control and regulation of snake antivenom immunoglobulins, WHO Press, Geneva, 2016. Available at: http://www.who.int/biologicals/ECBS_2016_BS2300_WHO_Guidelines_antivenom_clean1.pdf
- [37] D.J. Finney, Probit analysis; a statistical treatment of the sigmoid response curve. Macmillan, Oxford, England (1947). ISBN-13: 978-0521135900.
- [38] G.D. Laing, R.D.G. Theakston, R.P. Leite, W.D. Dias da Silva, D.A. Warrell, Butantan Institute Antivenom Study Group. Comparison of the potency of three Brazilian Bothrops antivenoms using *in vivo* rodent and *in vitro* assays. *Toxicon* 30 (1992) 1219-1225.
- [39] D.R. Rokyta, K.P. Wray, A.R. Lemmon, E.M. Lemmon, S.B. Caudle, A high-throughput venom-gland transcriptome for the Eastern Diamondback Rattlesnake (*Crotalus adamanteus*) and evidence for pervasive positive selection across toxin classes. *Toxicon* 57 (2011) 657–671.
- [40] D.R. Rokyta, A.R. Lemmon, A.R., Margres, M.J., Aronow, K. The venom-gland transcriptome of the eastern diamondback rattlesnake (*Crotalus adamanteus*). *BMC Genomics* 13 (2012) 312.
- [41] D.R. Rokyta, K.P. Wray, M.J. Margres, The genesis of an exceptionally lethal venom in the timber rattlesnake (*Crotalus horridus*) revealed through comparative venom-gland transcriptomics. *BMC Genomics* 14 (2013) 394.
- [42] M.J. Margres, K. Aronow, J. Loyacano, D.R. Rokyta, The venom-gland transcriptome of the eastern coral snake (*Micrurus fulvius*) reveals high venom complexity in the intragenomic evolution of venoms. *BMC Genomics* 14 (2013) 531.
- [43] J.J. McGivern, K.P. Wray, M.J. Margres, M.E. Couch, S.P. Mackessy, D.R. Rokyta, RNA-seq and high-definition mass spectrometry reveal the complex and divergent venoms of two rear-fanged colubrid snakes. *BMC Genomics* 15 (2014) 1061.
- [44] I.L.M. Junqueira-de-Azevedo, C.M. Bastos, P.L. Ho, M.S. Luna, N. Yamanouye, N.R. Casewell, Venom-Related Transcripts from *Bothrops jararaca* Tissues Provide Novel Molecular Insights into the Production and Evolution of Snake Venom. *Mol. Biol. Evol.* 32 (2015) 754-766.
- [45] F.J. Vonk, N.R. Casewell, C.V. Henkel, A.M. Heimberg, H.J. Jansen, R.J. McCleary, H.M. Kerkkamp, R.A. Vos, I. Guerreiro, J.J. Calvete, W. Wuster, A.E. Woods, J.M. Logan, R.A. Harrison, T.A. Castoe, A.P. de Koning, D.D. Pollock, M. Yandell, D. Calderon, C. Renjifo, R.B. Currier, D. Salgado, D. Pla, L. Sanz, A.S.

- Hyder, J.M. Ribeiro, J.W. Arntzen, G.E. van den Thillart, M. Boetzer, W. Pirovano, R.P. Dirks, H.P. Spaik, D. Duboule, E. McGlenn, R.M. Kini, M.K. Richardson, The king cobra genome reveals dynamic gene evolution and adaptation in the snake venom system, *Proc. Natl. Acad. Sci. USA* 110 (2013) 20651-20656.
- [46] R. Doley, N.N.B. Tram, M.A. Reza, R.M. Kini, Unusual accelerated rate of deletions and insertions in toxin genes in the venom glands of the pygmy copperhead (*Austrelaps labialis*) from Kangaroo island. *BMC Evol. Biol.* 8 (2008) 70.
- [47] D. Pla, D. Petras, A.J. Saviola, C.M. Modahl, L. Sanz, A. Pérez, E. Juárez, S. Fietze, P. Dorrestein, S.P. Mackessy, J.J. Calvete, Transcriptomics-guided bottom-up and top-down venomomics of neonate and adult specimens of the arboreal rear-fanged Brown Treesnake, *Boiga irregularis*, from Guam. *J. Proteomics* 174 (2018) 71-84.
- [48] N.R. Casewell, S.C. Wagstaff, W. Wüster, D.A.N. Cook, F.M.S. Bolton, S.I. King, S.I., D. Pla, L. Sanz, J.J. Calvete, R.A. Harrison, Medically important differences in snake venom composition are dictated by distinct postgenomic mechanisms. *Proc. Natl. Acad. Sci. U. S. A.* 111 (2014) 9205–9210.
- [49] J. Durban, A. Pérez, L. Sanz, A. Gómez, F. Bonilla, S. Rodríguez, D. Chacón, M. Sasa, Y. Angulo, J.M. Gutiérrez, J.J. Calvete, Integrated “omics” profiling indicates that miRNAs are modulators of the ontogenetic venom composition shift in the Central American rattlesnake, *Crotalus simus simus*. *BMC Genomics* 14 (2013) 234.
- [50] J. Durban, L. Sanz, D. Trevisan-Silva, E. Neri-Castro, A. Alagón, J.J. Calvete, Integrated Venomomics and Venom Gland Transcriptome Analysis of Juvenile and Adult Mexican Rattlesnakes *Crotalus simus*, *C. tzabcan*, and *C. culminatus* Revealed miRNA-modulated Ontogenetic Shifts. *J. Proteome Res.* 16 (2017) 3370-3390.
- [51] F.J. Joubert, A.J. Strydom, N. Taljaard, Snake venoms. The amino-acid sequence of protein S5C4 from *Dendroaspis jamesoni kaimosae* (Jameson's mamba) venom. *Hoppe-Seyler's Z, Physiol. Chem.* 359 (1978) 741–749.
- [52] O. Paiva, D. Pla, C.E. Wright, M. Beutler, L. Sanz, J.M. Gutiérrez, D.J. Williams, J.J. Calvete, Combined venom gland cDNA sequencing and venomomics of the New Guinea small-eyed snake, *Micropechis ikaheka*. *J. Proteomics* 10 (2014) 209-229.

- [53] L.P. Lauridsen, A.H. Laustsen, B. Lomonte, J.M. Gutiérrez, Toxicovenomics and antivenom profiling of the eastern green mamba snake (*Dendroaspis angusticeps*), *J. Proteomics* 136 (2016) 248-261.
- [54] S. Nirthanan, G.C. Gwee, Three-finger alpha-neurotoxins and the nicotinic acetylcholine receptor, forty years on. *J. Pharmacol Sci.* 94 (2004) 1-17.
- [55] R.M. Kini, R. Doley, Structure, function and evolution of three-finger toxins: mini proteins with multiple targets. *Toxicon* 56 (2010) 855-867.
- [56] Y.N. Utkin, Three-finger toxins, a deadly weapon of elapid venom—milestones of discovery. *Toxicon* 62 (2013) 50–55.
- [57] A. Bilwes, B. Rees, D. Moras, R. Menez, A. Menez, X-ray structure at 1.55 Å of toxin gamma, a cardiotoxin from *Naja nigricollis* venom. Crystal packing reveals a model for insertion into membranes. *J. Mol. Biol.* 239 (1994) 122–136.
- [58] R.M. Kini, Anticoagulant proteins from snake venoms: structure, function and mechanism. *Biochem J.* 397 (2006) 377-387.
- [59] A. Segura, M. Villalta, M. Herrera, G. León, R.A. Harrison, N. Durfa, A. Nasidi, J.J. Calvete, R.D.G. Theakston, D.A. Warrell, J.M. Gutiérrez, Preclinical assessment of the efficacy of a new antivenom (EchiTAb-Plus-ICP®) for the treatment of viper envenoming in sub-Saharan Africa. *Toxicon* 106 (2015) 97-107.
- [60] D.J. Williams, J.M. Gutiérrez, J.J. Calvete, W. Wüster, K. Ratanabanangkoon, O. Paiva, N.I. Brown, N.R. Casewell, R.A. Harrison, P.D. Rowley, M. O’Shea, S.D. Jensen, K.D. Winkel, D.A. Warrell, D.A. Ending the drought: New strategies for improving the flow of affordable, effective antivenoms in Asia and Africa. *J. Proteomics* 74 (2011) 1735–1767.
- [61] N.R. Casewell, I. Al-Abdulla, D. Smith, R. Coxon, J. Landon, Immunological cross-reactivity and neutralisation of European viper venoms with the monospecific *Vipera berus* antivenom ViperaTAb. *Toxins* 6 (2014) 2471–2482.
- [62] J.M. Gutiérrez, G. Solano, D. Pla, M. Herrera, A. Segura, M. Vargas, M. Villalta, A. Sánchez, L. Sanz, B. Lomonte, G. León, J.J. Calvete, J.J. Preclinical Evaluation of the Efficacy of Antivenoms for Snakebite Envenoming: State-of-the-Art and Challenges Ahead. *Toxins* 9 (2017), E163.
- [63] W. Wüster, S. Crookes, I. Ineich, Y. Mané, C.E. Pook, J-F. Trape, D.G. Broadley, The phylogeny of cobras inferred from mitochondrial DNA sequences: evolution of venom spitting and the phylogeography of the African spitting cobras (Serpentes: Elapidae: *Naja nigricollis* complex). *Mol. Phylogenet. Evol.* 45 (2007) 437–453.

- [64] European Directorate for the Quality of Medicines (EDQM). European viper venom antiserum. In: European pharmacopoeia 9.0. Strasbourg: EDQM; 2017, 1119-1120. <https://www.google.es/search?q=european+pharmacopoeia+9.0+pdf>.
- [65] X. Lou, X. Tu, G. Pan, C. Xu, R. Fan, W. Lu, W. Deng, P. Rao, M. Teng, L. Niu, Purification, N-terminal sequencing, crystallization and preliminary structural determination of atratoxin-b, a short-chain α -neurotoxin from *Naja atra* venom. *Acta Crystallogr D Biol. Crystallogr.* 59 (2003) 1038-1042.
- [66] F.J. Joubert, N. Taljaard, *Naja haje haje* (Egyptian cobra) venom. Some properties and the complete primary structure of three toxins (CM-2, CM-11 and CM-12). *Eur. J. Biochem.* 90 (1978) 359-367.
- [67] Kim, H.S., Tamiya, N. The amino acid sequence and position of the free thiol group of a short-chain neurotoxin from common-death-adder (*Acanthophis antarcticus*) venom. *Biochem. J.* 199 (1981) 211-218.
- [68] K. Kondo, H. Toda. K. Narita, C-Y- Lee, Amino Acid Sequences of Three β -Bungarotoxins (β 3-, β 4-, and β 5-Bungarotoxins) from *Bungarus multicinctus* Venom. Amino Acid Substitutions in the A Chains. *J. Biochem.* 191 (1982) 1531-1548.
- [69] S. Nirthanan, P. Gopalakrishnakone, M.C. Gwee, H.E. Khoo, R.M. Kini, Non-conventional toxins from Elapid venoms. *Toxicon* 41 (2003) 397-407.

Table 1. Comparison of the *A. s. intermedius* venom gland transcriptome and venom proteome expressed as percentages of toxin gene expression (transcriptome) and of protein abundance (proteome) of key toxin families identified. Green bars, toxin type is present at a higher relative frequency in the venom proteome than in the transcriptome; red bars, toxin type is present at a lower relative frequency in the venom proteome than in the transcriptome.



Table 2. Calculation of theoretical LD₅₀s of *Aspidelaps* venoms via the application of a toxicovenomics approach, and the reported LD₅₀s for major individual 3FTxs or 3FTx classes. *f*LD₅₀, fraction of the theoretical LD₅₀ contributed by the individual toxin listed in column "Toxin" and calculated as (%Toxinⁱ) x (LD₅₀ of Toxinⁱ). Percentages represent the relative abundance of the listed toxins (see pie charts displayed as panels B, D, and F of Fig.2).

Toxin	LD50 (μ g/g)	References	<i>A. s. intermedius</i>				<i>A. l. lubricus</i>		<i>A. l. cowlesi</i>	
			%	<i>f</i> LD50*	%	<i>f</i> LD50*	%	<i>f</i> LD50*	%	<i>f</i> LD50*
LNTx			28		40		41			
S ₄ C ₆	0.13	[17]	.9	0.038	.7	0.053	.8	0.054		
long α -NTx			2.				1.			
			3	0.003			9	0.0025		
CTx S ₃ C ₂	6.6	[18]	10		2.		4.			
			.5	0.693	1	0.138	8	0.317		
CTx S ₄ C ₈	9.4	[18]	23							
			.2	2,181						
PLA ₂			6.		5.		4.			
CM-II	1.1	[15]	1	0.067	7	0.063	9	0.054		

atratoxin			5.		25		22	
b	0.18	[65]	2	0.009	.6	0.046	.1	0.040
short			7.		1.		1.	
α NTxs	0.04-0.3	[54]	3	0.004-	4	0.0017-	6	0.002-
other			3.	0.032	2.	0.0126	3.	0.0153
α NTxs			5		8		5	
wNTx			1.					
CM-II	16.1	[66]	8	0.29				
α NTx			9.					
P01434	0.08	[67]	6	0.008				
β -NTx					2.		0.	
P81782	0.06-0.13	[68]			1	0.026	97	0.0012
					3.	0.16-	2.	0.11-
nc3FTx	5-80	[69]			1	2.48	1	1.68
				3.29-		0.49-		0.59-
Σ				3.31		2.82		2.16
Other			11		16		16	
toxins	(22)		.2	2.46	.5	3.63	.3	3.59
	Calculate			5.75-		4.12-		4.18-
	d LD50			5.77		6.45		5.75

* f LD50 = (%Toxin "i") x
(LD50 Toxin "i")

Table 3. Total and concentration-dependent immunoretained (RET) *A. l. cowlesi* (A) and *A. l. lubricus* (B) venom proteins by SAIMR polyvalent antivenom affinity column. Maximal binding for each RP-HPLC fraction is highlighted by yellow background.

--

ACCEPTED MANUSCRIPT

Fig. 1. The relative expression of transcripts encoding venom toxin classes identified in the *A. s. intermedius* venom gland transcriptome. The left pie chart shows toxin components with transcript abundances of >1% of all toxins, and the right pie chart shows a breakdown of components with <1% expression ('others'). For those toxins that are more abundantly expressed, the number of contigs encoding each toxin family are displayed in parentheses (for details, consult Supplementary Table S1). Key: three-finger toxin (3FTx), phospholipase A₂ (PLA₂), Kunitz-type inhibitor domains (KUN), cysteine-rich secretory protein (CRISP), C-type natriuretic peptide (C-NP), snake venom metalloproteinase (SVMP), nawaprin (NAW), nerve growth factor (NGF), hyaluronidase (HYA), vespryn (VSPN), serine proteinase (SP), 5'-nucleotidase (5'NUC), phosphodiesterase (PDE), cobra venom factor (CVF), dipeptidyl peptidase-4 (DPPIV), L-amino acid oxidase (LAO) and phospholipase B (PLB).

Fig. 2. Proteomic analyses of venom from three species of the genus *Aspidelaps*. Reverse-phase chromatographic separation of *A. s. intermedius* (Panel A), *A. l. lubricus* (Panel C) and *A. l. cowlesi* (Panel E) venom proteins. Insets, SDS-PAGE profiles of the various RP-HPLC isolated protein fractions analysed under non-reduced (upper gels) and reduced (lower gels) conditions. Pie charts displayed in panels B, D and F, show, respectively, the relative occurrence (in percentage of total venom proteins) of toxins from different protein families in the venoms of *A. s. intermedius*, *A. l. lubricus*, and *A. l. cowlesi*. PIII-SVMP, snake venom metalloproteinase of class PIII; svNGF, snake venom nerve growth factor; n.i., not identified; other acronyms as in the legend of Fig. 1.

Fig. 3. Immunological cross-reactivity between venom from *Aspidelaps* spp. and *Naja nivea* and the SAIMR polyvalent antivenom. A) Left panel: reduced SDS-PAGE gel electrophoretic profile of the four venoms; right panel: immunoblot of the SDS-PAGE with SAIMR polyvalent antivenom. B) End point titration curves showing the immunological binding between each venom and the SAIMR polyvalent antivenom with a five-fold dilution factor across the x-axis. C) Avidity titration curves showing the immunological binding between each venom and the SAIMR polyvalent antivenom in the presence of a chaotrope (ammonium thiocyanate), which is diluted across the x-axis. Key: ALL: *A. l. lubricus*; ALC: *A. l. cowlesi*; ASI: *A. s. intermedius*; NIV: *N. nivea*.

Fig. 4. Third-generation antivenomic analyses of *A. l. cowlesi* and *A. l. lubricus* venom with SAIMR polyvalent antivenom. Reverse-phase chromatographic analysis of whole venom (panel a) and of the non-retained and the immunoretained fractions recovered from affinity column (7 mg immobilised SAIMR antivenom F(ab')₂ molecules) incubated with increasing amounts (100-1200 µg) of venom from *A. l. cowlesi* (**A**) and *A. l. lubricus* (**B**) (panels b-i). Panels j-l, retained and non-retained venom fractions on mock matrix and naïve equine IgG affinity columns.

ACCEPTED MANUSCRIPT

Highlights

- The venom proteomes of *Aspidelaps scutatus* and *A. lubricus* subspecies were characterised.
- Consistent with the predominance of 3FTxs, murine envenoming by *A. s. intermedius* induced systemic neurotoxicity.
- Antivenomics analysis revealed extensively recognition of *Aspidelaps* venom toxins by the SAIMR polyvalent antivenom.
- The SAIMR antivenom neutralised the mouse lethal activity of *A. s. intermedius* venom with a potency of 0.235 mg venom/mL antivenom.
- Our data suggest that SAIMR antivenom could be a useful therapeutic tool against human envenomings by *Aspidelaps* species.

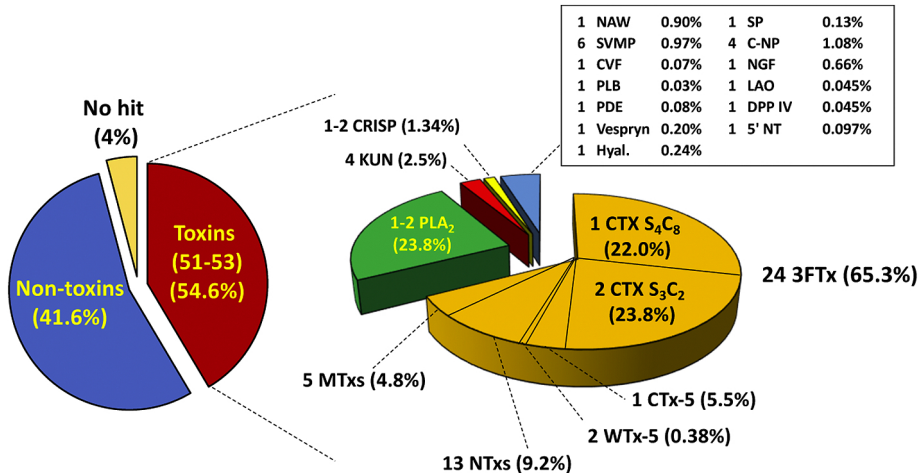


Figure 1

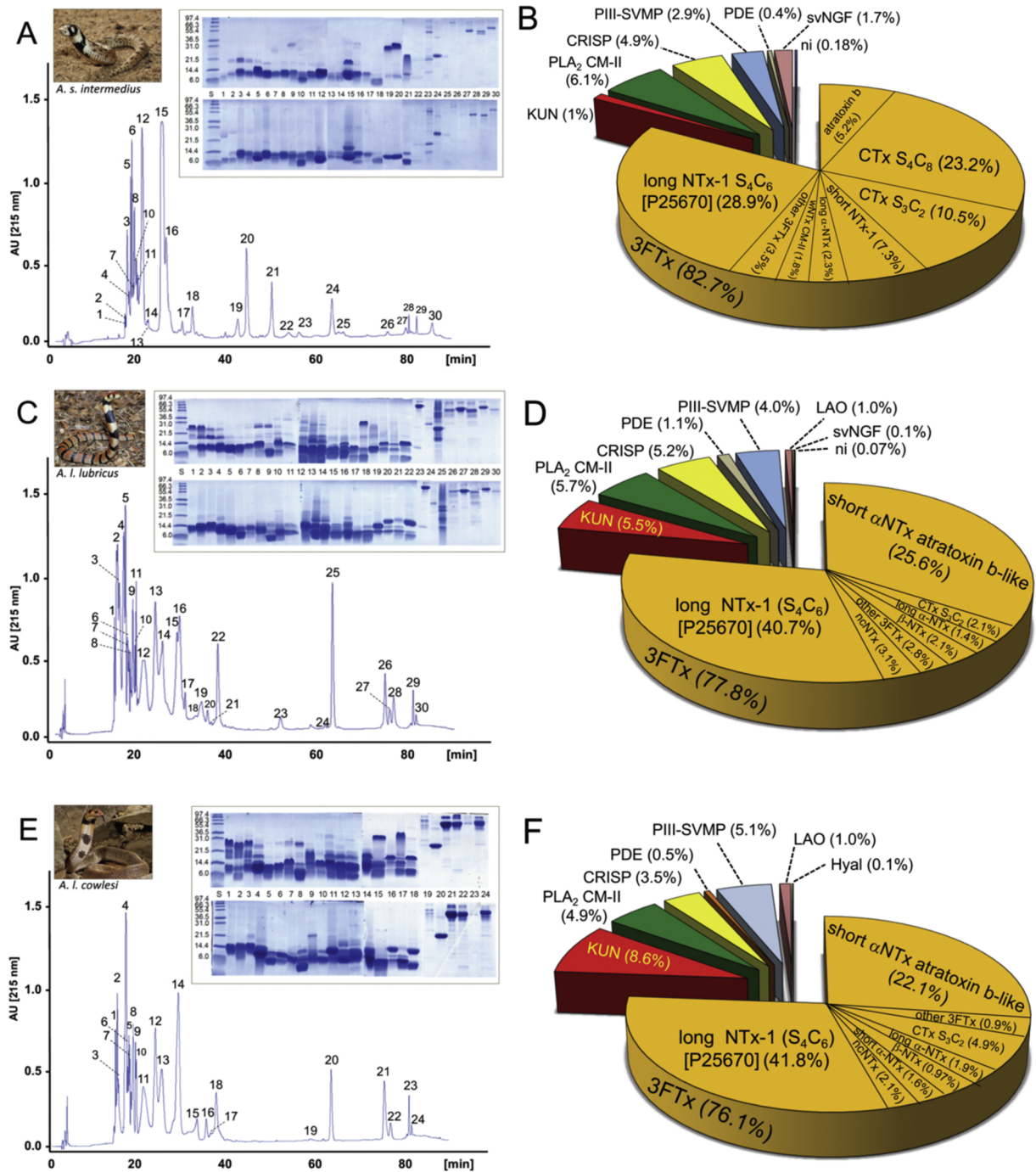


Figure 2

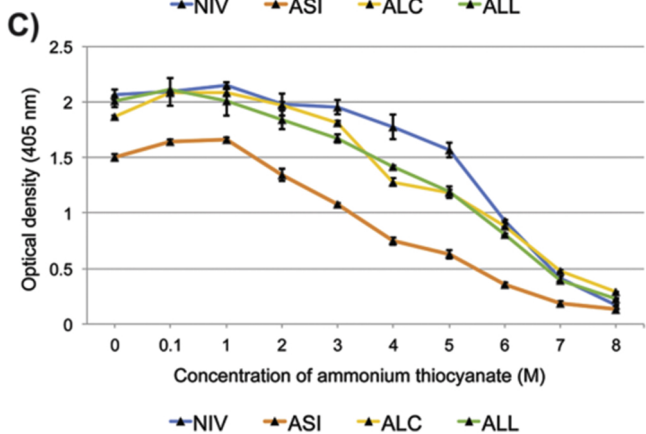
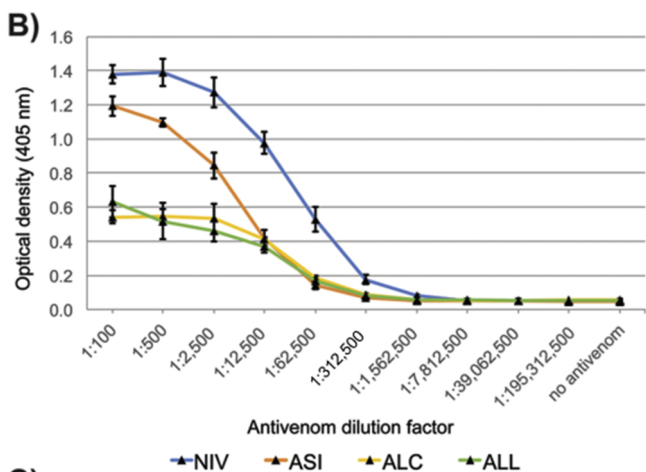
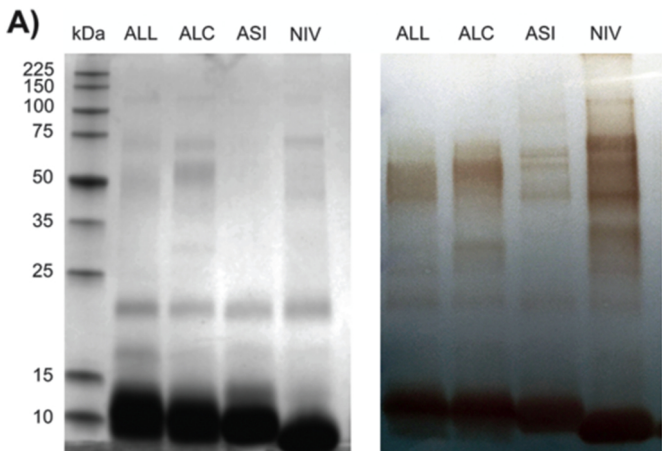


Figure 3

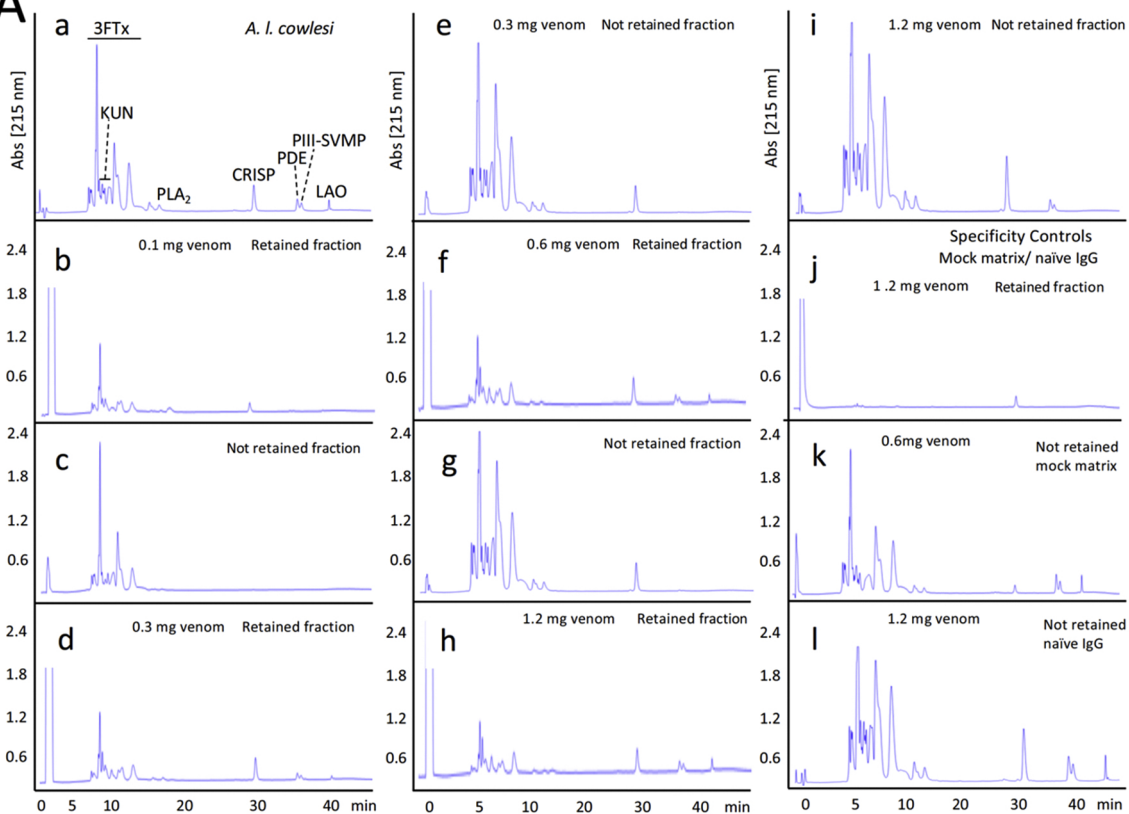
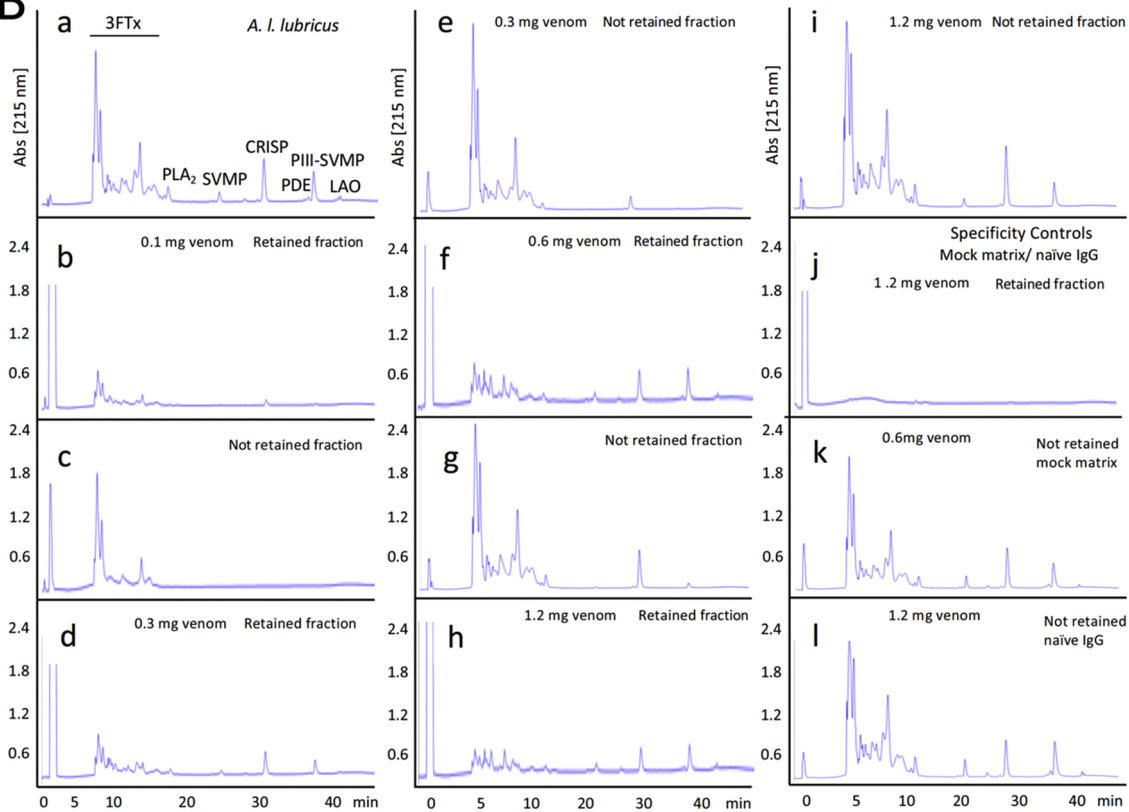
A**B**

Figure 4